Proceedings of the 21st ICSMGE, Vienna, Austria, 14 – 19 June 2026. Pistrol, Adam & Schweiger (eds.)
Published by: ÖGG, Austrian Society for Geomechanics, Salzburg, Austria, ISBN 978-3-9503898-4-5
https://doi.org/10.53243/ICSMGE2026-1012

Theoretical and full-scale experimental evaluation of 'installation friction' in self-drilling hollow piles

Juan Carlos Balbuena Ponce, Jean de Sauvage, Patrick Joffrin, and Jean-Pierre Rajot
Université Gustave Eiffel GERS/RRO, Lyon, France, juan-carlos.balbuena-ponce@univ-eiffel.fr

Philippe Robit and Anthony Martens
NGE Fondations, Lyon, France

ABSTRACT: The development of Prefabricated Diaphragm Walls (P. D. W.) inspired an innovative self-drilling hollow pile system to enhance efficiency in geotechnical construction. This study develops a novel numerical model to estimate axial friction during the installation of self-drilling hollow piles. The model, which simulates axial forces and bending moments under eccentric loading, is validated by comparing its predictions with compression forces measured during full-scale field tests. Results show an average axial friction of approximately 6 kPa for the first 8 meters of depth in cohesive soils, validated by a close convergence between modeled and measured compression forces. The proposed model effectively captures pile-soil interaction, offering a good initial framework for optimizing self-drilling hollow piles installation.

1 INTRODUCTION

Inspired by innovative solutions in underground retaining structures, NGE Foundations, in collaboration with the RRO Laboratory at Université Gustave Eiffel, developed an innovative self-drilling system to optimize the installation of prefabricated diaphragm walls. This system uses modular prefabricated bricks, each containing seven hollow cavities depicted in Figure 1 (a). A retractable drill head creates a 2-cm void space around the brick, reducing axial friction during installation. To investigate over-excavation's effect on axial friction, full-scaled field tests were conducted in clayey soil using 4-meter-long hollow pile elements, each simulating one cavity, measuring compression axial forces at element connections with three load sensors.

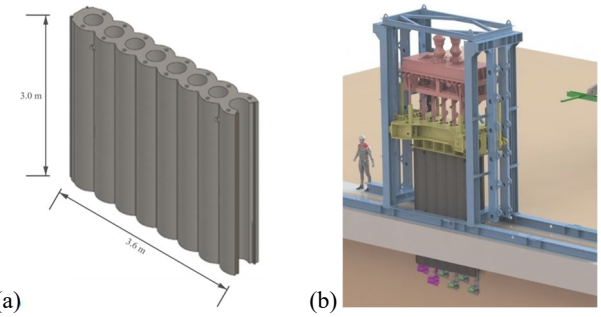

(a) (b)

Figure 1. Schematic representation of one modular prefabricated brick; (b) PREFO process installation for bricks using the self-drilling method.

Initial force equilibrium analysis revealed apparent negative friction values, indicating misinterpretation due to bending and tensile forces at connections. To address this, an inverse approach was adopted, incorporating an assumed friction law to predict compressive forces at connections. These predictions are then iteratively compared with field measurements, and the friction law is refined until convergence is achieved. The compressive forces are estimated using a numerical model based on Winkler and Hetényi beam-on-elastic-foundation approach, chosen for its suitability to simulate pile-soil interaction and bending moments under the eccentric driving loads.

This study presents the field testing, methodology, and results of evaluating installation friction in self-drilling hollow piles.

2 BACKGROUND AND OBJECTIVE

NGE Foundations is developing a new diaphragm wall construction system based on 3.6 × 3.0 m prefabricated elements. To optimize concrete consumption, the bricks are designed with hollow cavities. The PREFO process uses these spaces to house auger drills adapted with a retractable drill head. As the bricks are progressively assembled, the augers simultaneously over-excavates and extract soil, allowing the column to descend as shown in Figure 1 (b). Once the required depth is reached, the drill head retracts and is recovered through the hollow cavity. While this design enhances installation efficiency by creating a void around the brick, it also modifies the soil-element interface, consequently reducing the axial friction generated during installation.

The over-excavation method, similar to DPC piles, uses a retractable drill head to drill, extract soil, and drive elements downward (Chen et al., 2018; Hou et al., 2020). Unlike DPC piles, which use grout injection for lateral resistance (Tang et al., 2020; Hou et al., 2024), our method omits grouting, as diaphragm walls are designed to resist lateral soil pressure, not axial forces.

The key geotechnical challenge is to accurately quantify the axial skin friction that resists the installation of the prefabricated bricks. This friction increases over time, making driving more difficult. To study this soil-element interface, NGE Fondations designed hollow cylindrical elements that simulate the brick's individual cavities and replicate the over-excavation method.

3 FIELD TEST AND TECHNIQUE DESCRIPTION

Full-scale tests were conducted in clayey soil at Saint-Julien l'Ars, France, using four instrumented hollow piles. The piles, which were 4.0 m long and weighed 1.7 tons, had outer (D_e) and inner (D_i) diameters of 0.60 m and 0.30 m, respectively depicted in Figure 2 (a). The hollow elements are identified with the driving order progressing from Element No. 4 to No. 1, and were joined using a male-female coupling system with eight surrounding bolts as shown in Figure 2 (b).

As shown in Figure 3, an auger drilling rod with a retractable drill head passes through the hollow pile to be driven, all connected to a drilling machine. Once extended, the drill head provides a diameter of 0.64 m, resulting in a 2 cm over-excavation distance between the soil and the pile. The auger and the pile element are then connected to the machine,

and the driving process begins. Throughout the test, a free distance (h_f) between the drill head and the lower end of guide element No. 5 was maintained at 40 cm. After the initial guide element (No. 5) was driven, the remaining hollow piles were installed in the previously mentioned sequence. This process achieved a total depth of 20 meters.

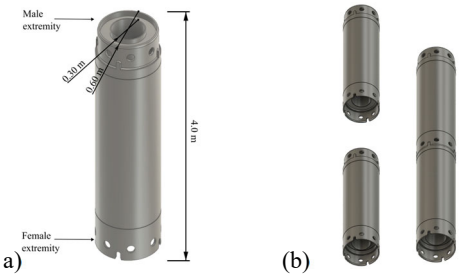

a) (b)

Figure 2. (a) Hollow pile dimensions and elements; (b) Connection procedure between hollow piles in the screw joint.

(a) (b)

Figure 3. The drill head in its (a) contracted and (b) extended states, under the hollow element No. 5.

During drilling, eight soil samples were taken to assess the composition and properties of the ground. Three main layers were identified (predominately clay soil). Atterberg limit tests were performed on several samples to analyze plasticity and moisture content.

4 METHODOLOGY

4.1 *Direct friction estimation*

Axial friction in self-drilling hollow piles is estimated using axial load differences, as direct measurement is not feasible. For the n^{th} element, $(F_{sup})_n$ and $(F_{inf})_n$ are reaction forces at the upper and lower parts, respectively, Figure 4 (a). In sequential driving, $(F_{sup})_n$ equals $(F_{inf})_{n-1}$ as shown in Figure 4 (b). Instant local axial friction is calculated via force equilibrium:

$$f_{s_n} = \frac{(F_{sup})_n + W - (F_{inf})_n}{A_n} \quad (1)$$

Where:

f_{s_n}: Instant local axial friction generated along the shaft of hollow element n, [kPa]

$(F_{sup})_n$: Total axial force recorded in the upper part of the element n, [kN].

$(F_{inf})_n$: Total axial force recorded in the lower part of the element n, [kN].

A_n: Area of the shaft in element n, calculated as $\pi \cdot D_e \cdot L_t$. Here, L_t varies with respect to the time/embedment depth, [m^2].

W: Weight of each element, equal to 17 kN

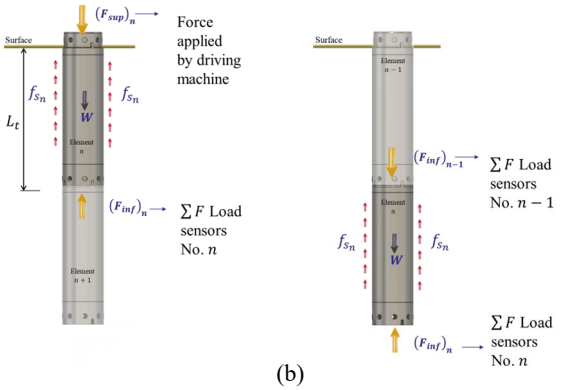

(a) (b)

Figure 4. Acting forces consideration in element n at two different instants, when: (a) the element is coupled to the machine and, (b) the element already driven and coupled to element $n-1$, in the male extremity.

This approach, termed the direct method, calculates friction directly from axial load measurements obtained during field tests.

4.2 *Instrumentation*

Three load sensors, positioned at 120° intervals within the female connection of each hollow pile element, were used to capture axial compression forces. These sensors were connected to a wireless micro-data logger, which recorded data at 100 Hz. The logger was activated before installation and turned off after the pile's extraction, at which point the data was downloaded. Knowing the precise location of each sensor allowed for detailed analysis of the load distribution. The axial force measurements are transmitted exclusively through the load sensors. Thus, when the machine applied pressure to the element the only point of contact is between the load sensors and the male extremity plate.

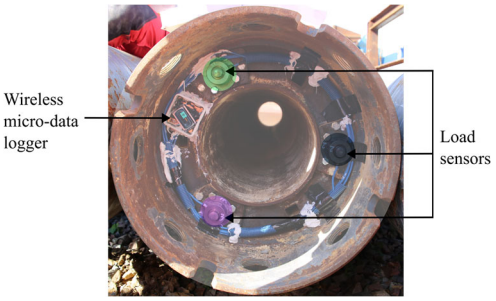

Figure 5. Instrumentation arrangement in hollow element, female extremity.

4.3 *Local friction estimation results*

Figure 6 display the instantaneous local friction, f_{s_n}, for the four hollow elements as a function of depth in two different ranges, from 0-3.5 m and from 3.5-7.5 m. The number of friction curves shown in the figures decreases with depth because fewer elements are present at greater depths. For instance, Figure 6 (a) shows all four elements, while Figure 6 (b) only shows elements No. 4, 3 and 2. A general decline in friction is observed in the first 3.5 m, but Figure 6 (b) also shows physically improbable negative friction values for elements No. 2, 3, and 4 at certain depths. These negative values are considered unreliable in the absence of consolidation.

A subsequent analysis revealed that the pile had a tendency to tilt during the entire driving process, causing tensile stress at the connections. This was confirmed by analyzing data from each of the three load sensors at every connection. This tilting effect was observed throughout the driving of all four elements.

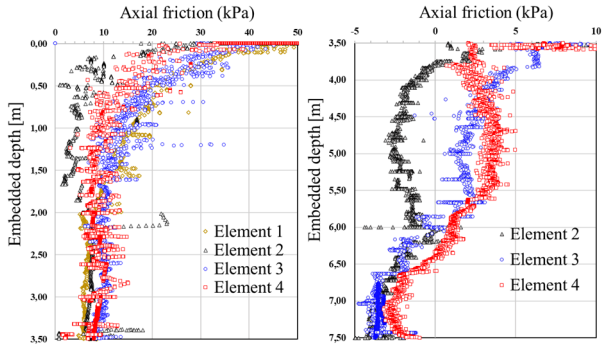

Figure 6. Local axial friction calculated based on direct method from (a) 0-3.5 m embedded depth and (b) 3.5-7.5 m

These results lead to two key assumptions. First, the load from the machine was eccentric, causing the pile to tilt. This induced bending moments and tensile forces at the connections. Second, the direct method cannot be applied because it doesn't account for these tensile forces. In fact, in Equation (1), the total force $(F_{\text{inf}})_n$ has to be broken down into known (measured by the load sensors) compression forces $\left(F_{C,\text{inf}}\right)_n$ and unknown tensile forces $\left(F_{T,\text{inf}}\right)_n$. To overcome this limitation, we developed an inverse method, which will be presented in the following chapter. This new approach is specifically designed to account for these forces.

5 FRICTION ESTIMATION: INVERSE APPROACH

This chapter presents a numerical model that uses an inverse method to estimate axial friction in self-drilling hollow piles. The method is an iterative process: it begins by assuming an initial friction law, then predicts compressive forces at pile connections, and compares these predictions with in-situ sensor measurements. The friction law is then adjusted repeatedly until the model's predictions converge with the measured data as explained in Figure 7.

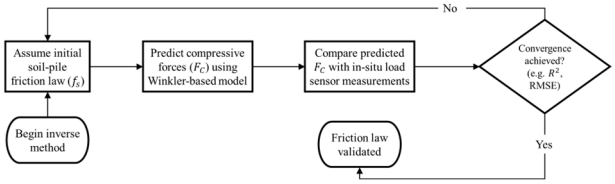

Figure 7. Flowchart of the inverse method for axial friction estimation

5.1 *Problem statement*

The model was initially developed for hollow element No. 4, reaching a total depth of 8.0 m. During driving, the element is subjected to an eccentric driving force, $F_M(t)$, which varies with time and induces an initial bending moment. The resulting stresses in the element are given by Equation (2):

$$\sigma_x = \frac{P(x,t)}{S} + \frac{M(x,t)}{I} y \tag{2}$$

Where, the $P(x,t)/S$ refers to the axial force at position x divided by the cross-sectional surface S, and $M(x,t)y/I$ the bending moment causing the element to tilt, divided by the second moment of area I of the hollow cross-section with respect to the centroidal axis equal to $I = (\pi/64)\left(D_e^4 - D_i^4\right)$, multiplied by y (any perpendicular distance from the neutral axis).

We are interested in evaluating the theoretical compression force F_C and comparing it with the obtained in the load sensors. Integrating Eq. (2) from y_n to R it is possible to obtain the compression force at any x:

$$F_c = \int_{y_n(x,t)}^{R} \left(\frac{P(x,t)}{S} + \frac{M(x,t)}{I} y\right) L(y)\, dy \tag{3}$$

Where $y_n = -P(x,t)I/[M(x,t)S]$ defined as the neutral axis where $\sigma_x = 0$ and $R = D_e/2$. Here $L(y)$ refers the chord length in the hollow pile's cross-section defined in (Balbuena Ponce et al., 2025).

For ease of analysis the most practical approach is to set the origin of the vertical axis x at the pile head, oriented downwards, where $L_1 = 4$ m, refers to the guide hollow pile and L_2 the length of the instrumented hollow element No. 4:

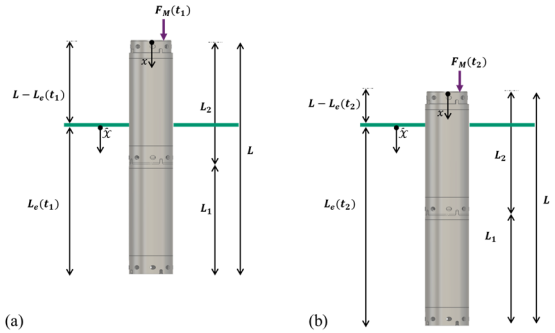

Figure 8. Pile axis alignment with a) $t = t_1$ and b) $t = t_2$

The ground surface at time t is defined as $x = L - L_e(t)$ and a new coordinate $\tilde{X}$ that starts at the ground surface and increases downward can be defined as $\tilde{X} = x - [L - L_e(t)]$:

Based on the Winkler beam-on-elastic-foundation model (Winkler, 1867; Hetényi, 1955; Heelis, Pavlović and West, 2004) and by applying equilibrium and Euler-Bernoulli beam theory (Beer et al., 2015), a fourth-order differential equation is derived:

$$EI\frac{d^4y}{dx^4} + f_s(x,t)\frac{dy}{dx} - \left[P_0 - \int_0^x f_s(x,t)\, dx\right]\frac{d^2y}{dx^2} + k_h(x,t)y = 0 \tag{4}$$

Here, E represents the Young's modulus of the hollow element equal to $E = 2 \times 10^8$ kPa. The model incorporates a soil reaction modulus, $k_h(x,t)$, that varies with depth and time (Rowe, 1956), the axial force, $P(x,t)$, is governed by the skin friction, $f_s(x,t)$, which is defined by:

$$P(x,t) = P_0 - \int_0^x f_s(x,t)\, dx \tag{5}$$

Where the border condition at the pile head $x = 0$ is equal to the force applied by the machine $P_0 = F_M(t)$.

5.1.1 *Boundary conditions*

At $x = 0$ the bending moment is calculated ad $M_0 = F_M(t) \cdot y_e$, where y_e refers to the eccentric distance y from the center where the resultant force F_M is applied.

The connection at $x = L_1$ to the guide pile imposes a rotational constraint with a maximum free inclination of θ_{max} =0.00015 rad. The connection acts as a linear rotational spring with stiffness k_r only when the absolute inclination $|dy/dx|$ equals or exceeds θ_{max}. Below this threshold, the bending moment at the connection is zero, indicating no rotational resistance defined as $M_{x=L_1} = -EI\frac{d^2y}{dx^2} = k_r\frac{dy}{dx}$.

At $x = L$, the pile tip is free of external moments and shear forces, as it is not constrained by additional connections at this point $M_{x=L} = -EI\frac{d^2y}{dx^2} = 0$, and the zero-shear condition is also valid in the pile's head $V_{x=0} = V_{x=L} = -EI\frac{d^3y}{dx^3} = 0$.

5.2 *Compression forces F_C comparison model vs in-situ*

To estimate friction, a numerical model was used to evaluate three constant unit friction values (f_s): 2 kPa, 6 kPa, and 8 kPa. The goal was to find the best match between the model's calculated compression forces (F_C) and in-situ measurements. Convergence was quantified using the coefficient of determination (R^2) and Root Mean Square Error (RMSE).

The results showed that f_s=6 kPa provided the best fit, with an R^2 of 0.1451 and an RMSE of 14.41. While this R^2 value is low, it represents the highest convergence among the cases tested. This limited fit is primarily attributed to the model's assumption of constant friction along the pile, as friction in actual conditions likely varies with depth due to changing soil properties. Figure 9 visually confirms that the modeled F_C values for f_s= 6 kPa align more closely with the in-situ data than the other values.

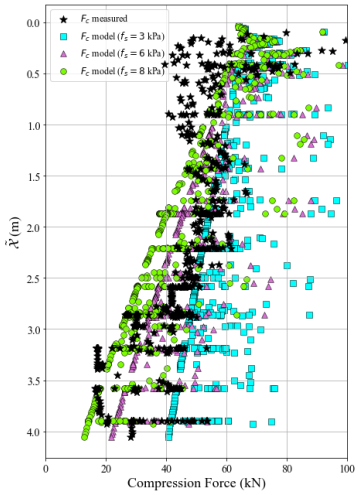

Figure 9. Compression force $F_C(4,t)$ profiles (measured in-situ vs model) in the embedded region at x = 4m at every instant for $f_s = 2$ kPa, $f_s = 6$ kPa and $f_s = 8$ kPa.

The f_s=6 kPa result could be interpreted using the α Method (Tomlinson, 1971), where $f_s = \alpha S_u$. With S_u estimated at 14.5 kPa from empirical correlations(Skempton, 1957; Bjerrum and Simons, 1960; Wroth and Houlsby, 1985) based on in-situ soil data (e.g., IP=28% and σ'_v=64 kPa), an adhesion factor α = 0.41 is required, lower than the expected α = 1. This suggests altered soil-pile interaction due to the over-excavation method, reducing adhesion compared to standard driven piles.

6 CONCLUSIONS

While the overarching innovation project involves the development of P. D. W., this work focuses on the critical installation phase the self-drilling hollow piles, which simulates the hollow, contiguous cavities within the prefabricated concrete bricks.

The direct method's limitations for instantaneous axial friction calculation led to a time- and space-dependent numerical model for self-drilling hollow piles. Validated by comparing predicted and measured compressive forces at pile connections, the model yields f_s = 6 kPa.

The next goal is to extend the model to include compressive forces from all four connections across the 20-meter length of self-drilling hollow piles. This further work will allow us to analyze the evolution of friction with depth and provide how the effects of soil remolding influence interfacial friction during the excavation.

The model's non-unique solutions depend on calibrating parameters like soil reaction modulus (k_h), rotational stiffness (k_r), and maximum rotation (θ_{max}). Further tests in diverse soil types are needed to enhance accuracy. To optimize the model for diverse soil conditions, an indirect optimization approach will calculate instantaneous axial friction by minimizing differences between theoretical and field-measured compressive forces using algorithmic methods. This will enable developing abacuses to estimate friction for various soil types, accounting for friction increases with depth due to cavity contraction and soil resistance.

7 ACKNOWLEDGEMENTS

The authors express their gratitude to NGE Fondations for their pioneering innovation in developing this novel self-drilling prefabricated pile technique, which forms the foundation of this study. Special thanks are extended to the technical team at the RRO Laboratory of Université Gustave Eiffel for their successful instrumentation efforts, which enabled the collection and interpretation of critical data. Finally, we acknowledge BPI France for their financial support, which made this research possible.

8 REFERENCES

Balbuena Ponce, J.C., de Sauvage, J., Joffrin, P., Rajot, J.-P., Robit, P. and Martens, A., 2025. Axial friction analysis of an innovative self-drilling prefabricated pile system: An inverse numerical method approach. *Submitted for publication*.

Beer, F.P., Johnston, E.R., DeWolf, J.T. and Mazurek, D.F., 2015. *Mechanics of Materials*. 7th ed. McGraw-Hill Education.

Bjerrum, L. and Simons, N.E., 1960. Comparison of shear strength characteristics of normally consolidated clays. *Proceedings of the ASCE Research Conference on Shear Strength of Cohesive Soils*, pp.711–726.

Chen, H., Hu, H., Tang, M., Yang, X. and Zhu, J., 2018. Hybrid Bored Prestressed Concrete Cased Piles: Equipment and Construction Procedures. *Journal of Construction Engineering and Management*, 144(12), p.06018006. https://doi.org/10.1061/(ASCE)CO.1943-7862.0001578.

Heelis, M.E., Pavlović, M.N. and West, R.P., 2004. The analytical prediction of the buckling loads of fully and partially embedded piles.

Hetényi, M., 1955. *Beams on Elastic Foundation: Theory with Applications in Engineering and Geology*. Ann Arbor, Michigan, U.S.A.: The University of Michigan Press.

Hou, Z., Liu, Y., Han, Z., Tang, M., Gong, X., Su, D. and Wang, L., 2024. Experimental Study of the Bearing Characteristics of a Novel Energy-Saving and Environmentally Friendly Pile: Drilling with Prestressed Concrete Pipe Cased Piles. *International Journal of Geomechanics*, 24(4), p.04024035. https://doi.org/10.1061/IJGNAI.GMENG-9062.

Hou, Z., Tang, M., Hu, H., Lin, Z., Chen, Y., Zhao, S. and Zhang, S., 2020. A new type of PHC pile-sinking technology: Drilling with PHC Pipe Cased Pile and its development directions. *IOP Conference Series: Earth and Environmental Science*, 580(1), p.012013. https://doi.org/10.1088/1755-1315/580/1/012013.

Rowe, P.W., 1956. The Single Pile Subject to Horizontal Force. *Geotechnique*, 6(4), pp.70–78. https://doi.org/10.1680/geot.1956.6.2.70.

Skempton, A.W., 1957. The planning and design of the new Hong Kong Airport. *Proceedings of the Institution of Civil Engineers*, 7(3), pp.383–389.

Tang, M., Hu, H., Cui, J., Yang, X., Hu, H. and Chen, H., 2020. The Vertical Bearing Mechanism of Hybrid Bored Pre-stressed Concrete Cased Piles. *International Journal of Civil Engineering*, 18(3), pp.293–302. https://doi.org/10.1007/s40999-019-00466-7.

Tomlinson, M.J., 1971. Some effects of pile driving on skin friction. In: *Behaviour of piles*. Thomas Telford Publishing. pp.107–114.

Winkler, E., 1867. Die Lehre von der Elasticitaet und Festigkeit [The theory of elasticity and strength]. *Dominicus: Prag*.

Wroth, C.P. and Houlsby, G.T., 1985. Soil mechanics and foundation engineering. *Geotechnique*, 35(2), pp.169–219.